COMPRESSION AND ASSOCIATED PROPERTIES OF BORON CARBIDE

D. P. Dandekar*and J. A. Ciezak
Army Research Laboratory, APG, MD 21005

M. Somayazulu
Geophysical Laboratory, Carnegie Institution of Washington, Washington, DC 20015

ABSTRACT

Our present work presents a direct association of the observed loss of shear strength in boron carbide under plane shock wave compression to amorphization in boron carbide under triaxial stress compression. This evidence is obtained from in-situ measurement of Raman, and infrared vibrational spectra of boron carbide confined in a Diamond Anvil Cell (DAC) under hydrostatic and non-hydrostatic pressures to 50 and 23 GPa, respectively. X-ray-diffraction measurements do show a shift in the compression of boron carbide around 27 GPa. However, X-ray diffraction measurements indicate that the amorphization does not extend to μm scale, as there is no evidence of a loss of crystallinity in the recorded diffraction pattern of boron carbide to 47 GPa. Our work shows that shear plays a very dominant role in the stress-induced amorphization of boron carbide.

1. INTRODUCTION

Boron carbide is a potentially attractive material for lightweight armor. Its high strength, hardness, and melting temperature also make it ideally suited for use as an abrasive material capable of sustaining extreme conditions of high-pressures and temperatures. The current understanding is that the performance of a ceramic, as a protective element, under impact loading may be critically dependent on retention or increase in the shear strength under compression (Bourne, 2008). This is the case even though ceramics generally fail under a small tensile stress due to their inherent low ductility. In boron carbide, the hardness and refractory nature relates to the strong C-B-C bonds in the network of linked icosahedra, the substitution of which can vary according to the carbon/boron ratio of the sample. The most accepted model for the rhombohedral structure of boron carbide considers $B_{11}C$ icosahedra clusters linked by a C-B-C chain along the main diagonal of the rhombohedron, as is shown in Figure 1. Elemental excess of either boron or carbon results in variation in the stoichiometry of the sample: excess carbon often results in the substitution of carbon for boron atoms within both $B_{11}C$ icosahedra and the C-B-C chains and causes graphitic regions to form in the sample, whereas excess boron results in regions of β-rhombohedral boron.

Analysis of existing shock compression data on boron carbides, irrespective of stoichiometry, impurities, and processing technique, indicate that Boron Carbides suffer a loss of shear strength when shocked above its Hugoniot Elastic Limit (HEL), i.e., 17-20 GPa (Dandekar, 2001). The loss of shear strength was suggested to be due to heterogeneous deformation of boron carbide, such as propagation of cracks, cleavages, heterogeneous melting zones, or/and a phase transition. Subsequently, when recovered fragments of boron carbide shocked beyond the HEL were examined by means of TEM and HERM by Chen et. al. (2003), they found evidence of amorphous phase in boron carbide fragments. Therefore, Chen et. al. (2003) suggested that the observed loss of shear strength under plane shock wave compression may be partly due to the formation of an amorphous phase transition near these pressures. Several other static and dynamic indentation studies also show evidence of amorphization in boron carbide at comparable stresses under static and dynamic indentations (Ge et. al. 2004; and Ghosh et. al. 2007). The evidence for amorphization phase transition in B_4C was obtained by the means of TEM, HERM, Raman, and Infrared spectra.

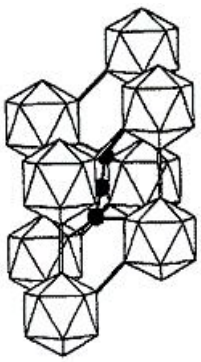

Figure 1. Crystal structure of boron carbide (B_4C)

Report Documentation Page

Form Approved
OMB No. 0704-0188

1. REPORT DATE	2. REPORT TYPE	3. DATES COVERED
DEC 2008	**N/A**	**-**

4. TITLE AND SUBTITLE	5a. CONTRACT NUMBER
Compression And Associated Properties Of Boron Carbide	5b. GRANT NUMBER
	5c. PROGRAM ELEMENT NUMBER
6. AUTHOR(S)	5d. PROJECT NUMBER
	5e. TASK NUMBER
	5f. WORK UNIT NUMBER
7. PERFORMING ORGANIZATION NAME(S) AND ADDRESS(ES) **Army Research Laboratory, APG, MD 21005**	8. PERFORMING ORGANIZATION REPORT NUMBER
9. SPONSORING/MONITORING AGENCY NAME(S) AND ADDRESS(ES)	10. SPONSOR/MONITOR'S ACRONYM(S)
	11. SPONSOR/MONITOR'S REPORT NUMBER(S)

12. DISTRIBUTION/AVAILABILITY STATEMENT
Approved for public release, distribution unlimited

13. SUPPLEMENTARY NOTES
See also ADM002187. Proceedings of the Army Science Conference (26th) Held in Orlando, Florida on 1-4 December 2008, The original document contains color images.

14. ABSTRACT

15. SUBJECT TERMS

16. SECURITY CLASSIFICATION OF:			17. LIMITATION OF ABSTRACT	18. NUMBER OF PAGES	19a. NAME OF RESPONSIBLE PERSON
a. REPORT	b. ABSTRACT	c. THIS PAGE			
unclassified	**unclassified**	**unclassified**	**UU**	**8**	

The appearance of the amorphous phase in boron carbide is strongly associated with the emergence of three vibrational peaks between 1200 cm^{-1} and 1700 cm^{-1} in the spectra near 18 GPa (Chen et. al., 2003; Ge et. al., 2004; Ghosh et. al. 2007). This includes: (i) a disorder-induced (D) carbon peak near 1335 cm^{-1}, (ii) a weak graphite peak (G) near 1590 cm^{-1} which has been attributed to the presence of free carbon associated with the non-compressed polycrystalline B_4C, and (iii) and an unidentified peak near 1800 cm^{-1}. The emergence of the D and G peaks suggests the amorphization involves localized formation of sp^2 hybridized aromatic C rings and implies that the observed amorphization is due to formation of amorphous carbon (a-C) clusters in the statically indented region. In contrast, the observed amorphization in the dynamically indented region was correlated to the formation of both a-C and amorphous boron (a-B) clusters (Ghosh et. al., 2007). Formation of a-B clusters was suggested from the weakening of the vibrational intensities of the features near 1100 cm^{-1} and 1590 cm^{-1}, which correspond to the B-C stretching vibration and the C-B-C chain stretch, respectively. Additionally, a new band appeared after dynamic indentation between 760 cm^{-1} and 830 cm^{-1}, which has also been correlated with the amorphous transition (Ghosh et. al., 2007).

In contrast to the vibrational data, x-ray diffraction studies performed under high-pressure have yet to reveal any large structural changes. This suggests that amorphization in boron carbide is not massive (Somayazulu et. al., 2001).

The previous static and dynamic compression and indentation studies found evidence of amorphization in boron carbide upon examination under the released stress condition i.e., the evidence for amorphization was not obtained while boron carbide was under compressed state. On the other hand, the loss of shear strength in boron carbide is observed in the shock wave induced compressed state; thus, the observed loss in the shear strength could not be directly attributed to the observed amorphization in the released stress state of boron carbide. As a result, it was necessary to seek evidence of amorphization in boron carbide under an appropriate compressive stress state. Further, since all the investigations related to the loss of shear strength were performed under non-hydrostatic pressure conditions, the current experimental investigation on boron carbide was initiated to examine:
(i) Is the triaxial compressive stress environment necessary for initiating amorphization in boron carbide?
(ii) Is the amorphization in boron carbide initiated during the compressive stress state?

To answer these two questions, the x-ray diffraction, and Raman and Infrared spectra were obtained in a compression sequence in both hydrostatic and non-hydrostatic pressure environments. These measurements were undertaken in an effort to understand the relationship between the compressive state and the initiation of amorphization in boron carbide.

2. MATERIALS AND EXPERIMENTAL METHODS

Piston-cylinder type diamond anvil cells with 300 μm diamond culets were used for all static high-pressure experiments. The polycrystalline boron carbide samples, with a stoichometric ratio of $B_{4.3}C$ (~ B_4C), were obtained from CERCOM and used without further purification. For all high-pressure experiments, a 60-100 μm B_4C sample was loaded into the sample well (~ 120μm in diameter) of a rhenium gasket. Additionally, for one group of Infrared experiments, the B_4C sample was ground for several minutes between the two diamond anvils. To test the effect of hydrostatic conditions on the high-pressure behavior of B_4C, the experiments used both non-hydrostatic (NH) and hydrostatic conditions. Hydrostatic conditions were generated using a helium pressure medium, which was loaded into the diamond anvil cell using a specialized high-pressure gas system described elsewhere (Mao et al, 1986). The pressure within the diamond anvil cell was determined from the frequency shift of the ruby R_1 fluorescence line (Zha et al. 2000). The position and widths of both the R_1 and R_2 luminescence lines of ruby were monitored as a function of pressure to estimate the hydrostaticity of the sample. Raman spectra were obtained from an Ar^+ ion laser operating at 514.5 nm with an optical system previously described (Goncharov et al., 1998) and a laser spot diameter of ~ 4 μm at room temperature. Prior to any experimental measurements, a wavelength calibration of the spectrograph was performed with a Neon lamp; this method of calibration has an accuracy of ±1 cm^{-1}. The spectral resolution for all Raman measurements was ± 4cm^{-1}. High-pressure synchrotron infrared absorption measurements were obtained at beamline U2A of the National Synchrotron Light Source (NSLS) of Brookhaven National Laboratory (BNL) with the light extracted from the x-ray source in a method previously described (Liu et al., 2002). A spectral resolution of 4 cm^{-1} was used for all IR measurements. The energy dispersive X-ray diffraction experiments were conducted to 24 GPa employing a neon pressure medium at X17C of the NSLS at Brookhaven National Laboratory (Hu et al., 1994) with a wavelength of 0.41Å.

3. RESULTS AND DISCUSSION

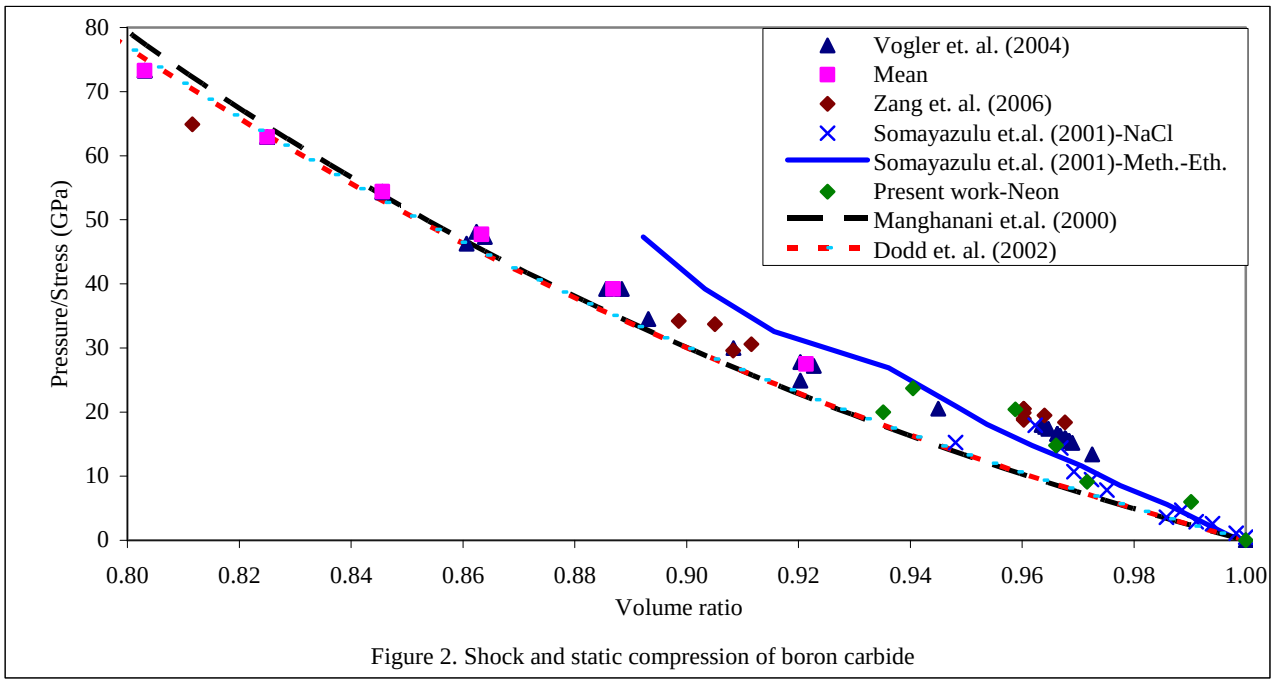

Figure 2. Shock and static compression of boron carbide

3.1 Compression

Compression of CERCOM boron carbide under shock, and static compression has been investigated by Vogler et. al. (2004), and Somayazulu et. al. (2001) and Dodd et. al. (2002), respectively. Somayazulu et.al. (2001) used NaCl and 4:1 methanol-ethanol mixture as the pressure media and neon was used in the current work to determine static compression of boron carbide from x-ray diffraction measurements. Dodd et. al. (2002) measured pressure dependences of elastic properties of boron carbide. Zhang et. al. (2006) reported shock compression of 99.9% pure boron carbide. Manghanani et. al. (2000) reported compression of a fully dense B_4C synthesized at the Dow Chemical. The results of pressure volume compression of boron carbide from these investigations and the current work are shown in Figure 2.

Figure 2 shows that the hydrostatic compression curves of boron carbides obtained by Manghanani et. al. (2000) and Dodd et. al. (2002) from ultrasonic wave velocity measurements at high pressures are identical. Similarly, the difference between the shock induced compression of boron carbides determined by Vogler et. al. (2004) and Zang et. al. (2006) is not significant. The loss of shear strength in boron carbide above the HEL is evident from the negligible differences between shock and mean stress coordinates around 30 GPa and beyond. Another significant fact that emerges from this figure is that static compression data obtained from the x-ray diffraction investigations, i.e., Somayazulu et.al. (2001) and the present work lies on the elastic deformation loci of the shock compression to around 27 GPa. This is the case even though three different pressurizing media with varying shear strength under pressure, i.e., NaCl, 4:1 methanol-ethanol, and neon, were used to confine boron carbide in the diamond anvil cell (DAC) in the x-ray diffraction experiments. This suggests that the pressure environment in the static experiments was non-hydrostatic. The reason for the above is not clear at present and remains to be investigated. However, it has an unexpected benefit. The measured pressure for the onset of amorphization and related changes in the Raman and Infrared spectra of boron carbide observed in our experiments would be close to the shock induced stress in boron carbide. None of the high-pressure x-ray diffraction experiments showed any evidence of a phase transition i.e., amorphization of boron carbide, to 47 GPa as shown in Figure 3. It implies that the long-range order is on an average preserved at the micron level in boron carbide. The values of hexagonal lattice parameters a and c at ambient conditions were determined to be 0.5606 and 1.2087 nm, respectively. This implies that the atomic ratio of boron and carbon was 4:1 (Aselage and Emin, 1991).

It should be mentioned that a shift in the compression curve observed by Somayazulu et. al. (2001) around 27 GPa suggests an onset of softening of compression of boron carbide. The shift in compression curve of boron carbide appears to be due to a shift in the value of basal lattice parameter of the hexagonal lattice of boron carbide around 27 GPa. The other lattice

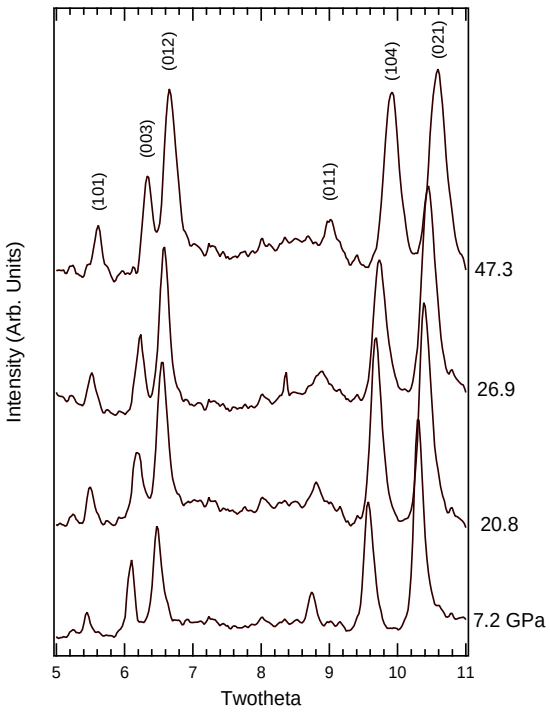

Figure 3. Representative diffraction patterns of B_4C in 4:1 methanol-ethanol pressure medium. The data was obtained with a monochromatic incident beam set at 0.4246 A. The background from each pattern has been subtracted (Somayazulu et. al. (2001).

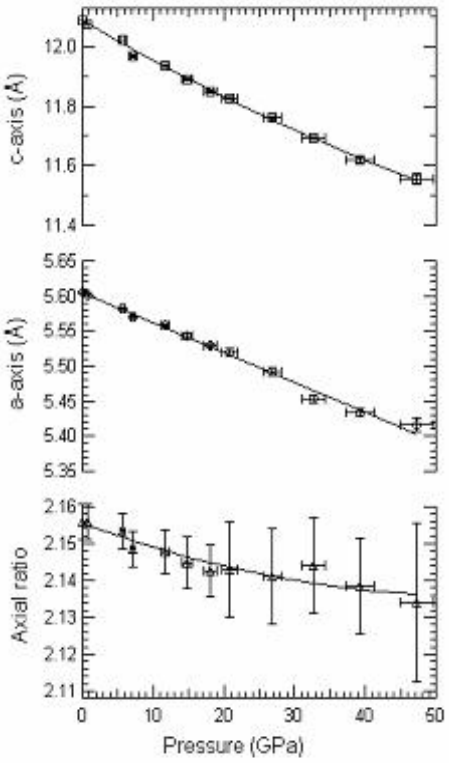

Figure 4. Cell lengths and axial ratio of boron carbide as a function of pressure (Somayazulu et. al. (2001).

parameter changes smoothly over the whole pressure range (Figure 4). The underlying mechanism for the observed shift remains to be identified.

3.2 Vibrational Spectra

The Raman and Infrared spectra of normal B_4C to pressures of 50.1 GPa and 23.1 GPa, respectively are presented in Figure 5. The spectra of the former were obtained using both hydrostatic (helium) and non-hydrostatic (boron carbide) pressure media while the spectra of the latter, due to experimental constraints were obtained only under non-hydrostatic conditions. The Raman spectra at 50.1 GPa reveal a number of broad low-frequency bands associated with the internal vibrational modes of B_4C molecules in accordance with previous studies at high pressures (Manghanani et. al. 2000, Yan, et al., 2006 and references therein). Infrared spectra obtained to 23.1 GPa are also in good agreement with earlier experimental studies performed at lower pressures (Lazzari, et al., 1999, Werheit et al., 1999). Table 1 summarizes the Raman and Infrared frequency bands that appear within this pressure range and includes the corresponding frequency shifts with pressure. The Raman modes centered near 268 cm^{-1} and 328 cm^{-1} show a slight mode softening as a function of pressure. These modes arise from rotation of the icosahedra and C-B-C chain, respectively (Shirai, et al., 1996) and are characterized by strong covalent bonding. The relatively small shift in the vibrational frequencies as a function of pressure reflects the strong covalent interaction and the rigid bonding structure associated with these modes. While speculative, the softening likely arises from a subtle distortion of the B_4C structure not apparent in the x-ray diffraction.

The Raman spectra obtained with the helium and non-hydrostatic pressure media are qualitatively very similar below 1200 cm^{-1}. However, two broad features also appear in the non-hydrostatic spectra ca. near 1630 cm^{-1} and 1750 cm^{-1}. A comparison of the frequencies of the IR bands with those of the Raman spectrum suggest that they originate from the graphitic impurity inherent to all B_4C samples (1630 cm^{-1}) and as well as an amorphous B_4C phase (a-B_4C) (Yan et al., 2006). It has to be noted that the vibrational position of the graphite peak in the Raman spectra occurs at a slightly higher frequency than the 1500-1600 cm^{-1} range that was reported in previous works (Yan et al., 2006, Domnich, et al., 2002; Ghosh, et al., 2007). Because the synthesis methods of B_4C make each batch unique, the shift in the graphite frequency originates from differing ratios of the sp^2/sp^3 bonding in graphite and amorphous carbon. The graphite and a-B_4C vibrational features appear at slightly different frequencies in the Infrared and Raman due to differing selection rules.

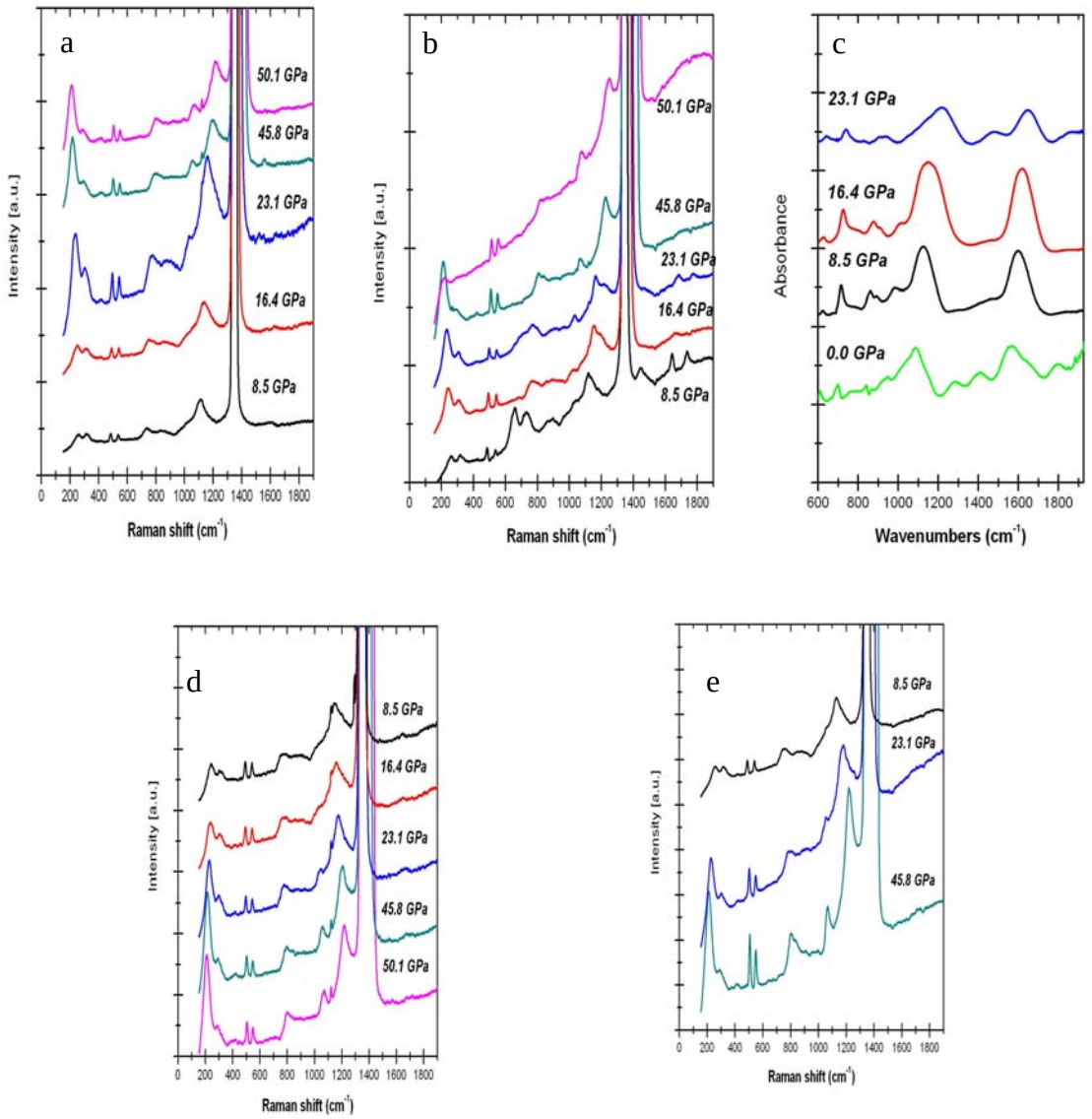

Figure 5. Vibrational spectra of boron carbide shown as a function of pressure: Raman compression sequence with (a) helium pressure medium and (b) non-hydrostatic conditions, (c) Infrared compression sequence with non-hydrostatic conditions and Raman decompression sequence with (d) helium pressure medium and (e) non-hydrostatic conditions.

Of particular interest in the Raman and Infrared spectra is the vibrational band that appears between 1730 cm^{-1} and 1800 cm^{-1}. The exact origin of this feature is unknown, although several experimental studies have used its development in the vibrational spectrum as a key indicator of the formation of an amorphous B_4C phase (Domnich, et. al. 2002, Ge et. al. 2004, Yan et al., 2006). Since this band appears in the Raman spectra collected under non-hydrostatic compression and not in the hydrostatic Raman spectra, we can correlate its appearance with the existence of deviatoric stress present in the non-hydrostatic sample. This implies that the amorphization process is strongly governed by the triaxiality of stress state on the sample. It is interesting to note the a-B_4C feature appears at pressures as low as 8.5 GPa since previous experimental measurements have suggested the transition occurs between 18-21 GPa (Yan et al., 2006, Domnich, et al., 2002; Ghosh, et al., 2007). Although the peak is well resolved at lower pressures, over the pressure range studied, the peak broadens and loses intensity. At the highest pressures studied (50.1 GPa), the vibrational maxima encompasses both the lower frequency graphitic peak

Table 1. Vibrational frequencies of Boron Carbide. Ref. a. Shirai, et al., 1996, b. Yan et al., 2006, c. Werheit et al., 1999, d. Schneider et al., 1995.

Raman			*Infrared*				*Mode assignment*
Ambient pressure (cm^{-1})	**Helium $d\nu/dP$**	**Non hydrostatic $d\nu/dP$**	**Ambient pressure (cm^{-1})**	**Pure $d\nu/dP$**	**Ambient pressure (cm^{-1})**	**Ground $d\nu/dP$**	
268	-1.5	-0.9					Rotation of icosahedra [a]
328	-0.8	-1.2					Rotation of C-B-C chain [a]
479	0.4	0.7					C-B-C chain stretch [b]
532	0.4	0.4					liberational mode of $B_{11}C$ isosahedra [b]
			609	1.3	644	4.2	Unknown [c]
655	NR	2.3					overtone 2 X 328 cm^{-1}
722	1.8	2.5	699	1.8	730	0.2	Intraicosahedral/ interiscosahedral breathing [b]
867	2.1	NR	842	2.8	886	0.2	Intraicosahedral/ interiscosahedral breathing [b]
			943	-0.3	1018	-0.4	C-B-C chain stretch and icosahedra rotation about C-B-C bond [c]
1001	1.3	1.6					chain rotation [b]
1091	2.6	2.7	1087	5.8	1175	0.8	Icosahedra breathing mode [b]
			1282	2.9	1374	0.2	Disordered graphite[d]
1446	NR	1.9	1418	5.1	1506	0.4	combination band ~1088 cm^{-1} + ~330 cm^{-1}
1647	NR	* evolve into a single feature	1567	3.5	1626	0.2	free carbon in B_4C [b]
1734	NR		1797	3.3	1873	-0.4	Unknown but thought be related to amorphization [b]

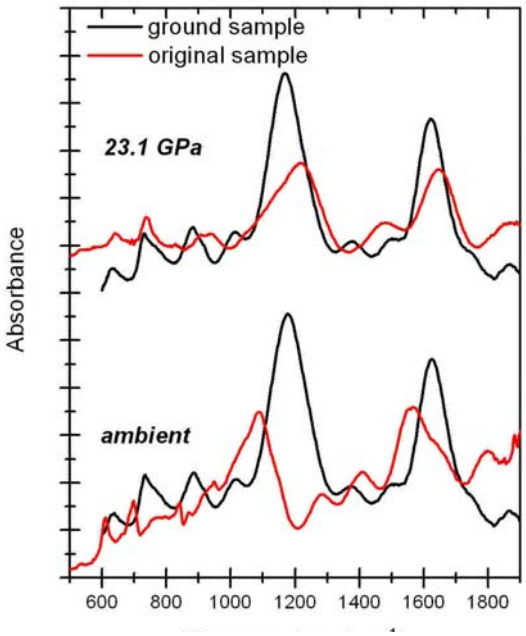

Figure 6. Infrared spectra of normal and ground boron carbide at ambient and 23.1 GPa.

and the a-B_4C feature. The loss of resolution and significant increase in the vibrational line width is consistent with a decrease in crystalline long-range order on 1-10 nm scale. However, since there is little variation in the line width of many lower frequency vibrations, we suggest the amorphization is highly localized rather than encompassing the entire sample. Further, there is a significant decrease in the intensity of the peaks located near 270 cm^{-1} and 320 cm^{-1} between 46 GPa and 50 GPa under non-hydrostatic conditions, while under hydrostatic conditions the intensity remains fairly constant over this pressure range. The vibrational assignment of these two features and their correlation to the ~1800 cm^{-1} feature is unclear, but similar peaks in boron arsenide have been associated with icosahedron-chain modes (Tallent et al., 1989). Therefore, we tentatively assign these features in B_4C to icosahedron-chain modes. In boron arsenide, the intensity of these modes was found to be immensely sensitive to the crystalline orientation and a correlation can be made to the intensity decrease of these features in boron carbide. It suggests that the material disorders along the C-B-C plane, a result that is consistent with previous suggestions (Yan et al., 2006) and TEM results. This type of structural disorder is very subtle and detection may be beyond the diffraction limit as evident from the results of high pressure x-ray diffraction experiments on boron carbide (Somayazulu, et al., 2001, and current work). Thus, crystallographic evidence of an amorphous phase has remained elusive.

In an attempt to induce the amorphous boron carbide transition at ambient conditions, a small sample was ground within the diamond anvils prior to IR characterization. Infrared measurements were chosen over Raman for this characterization because IR has greater sensitivity to small structural changes as a result of slight dipole changes. Figure 6 shows a comparison of the infrared spectra of the original pure and ground samples at both ambient pressure and 23.1 GPa. At ambient pressure, the ground sample shows a significant shift towards higher frequencies. As can be seen from Figure 6 and Table 1, the ground sample also shows less of a pressure-induced shift on the frequencies than the original sample. Although the exact cause of this shift is unclear, it likely results from a lowering of the barrier to transition, similar to calcium carbonate (Liu, et al., 1990; Davis, 1964). At higher pressures, the ground and original samples show nearly identical features, although the resolution is greatly enhanced in the ground sample. This method may be a viable way to obtain the x-ray diffraction since much larger samples can be made at ambient conditions, and one is not limited by the geometry of the diamond anvil cell. Further studies are currently in progress to determine the crystallographic structure of the ground sample.

CONCLUSIONS

The results of the current work may be summarized as follows:

(1) A shift in compression of boron carbide with pressure above the HEL, around 23 GPa, appears to be partly associated with the change the basal lattice parameter 'a' of boron carbide.

(2) The initiation of amorphic changes in crystalline boron carbide is observed to occur at as low as 8 GPa under non-hydrostatic pressure/stress environment. No evidence of amorphization is present when boron carbide is compressed hydrostatically to 50 GPa. The observed loss of shear strength in boron carbide under plane shock wave compression can be associated with the amorphization in it. If so, the effect of amorphization on the compression of boron carbide is negligible until the global stress exceeds the HEL.

(3) The only modes that indicate a softening with pressure are those centered near 268 cm^{-1} and 328 $cm^{-1.}$ These modes arise from rotation of the icosahedra and C-B-C chain, respectively [Shirai, et al., 1996] and are characterized by strong covalent bonding. The relatively small shift in the vibrational frequencies as a function of pressure reflects the strong covalent interaction and the rigid bonding structure associated with these modes. We suggest the observed softening arises from a subtle distortion of the B_4C structure not apparent in the x-ray diffraction.

(4) Not surprisingly, our infrared spectra do not indicate any evidence of formation of a-B clusters as found under dynamically indented boron carbide (Ghosh et. al., 2007). As such, we do not see any weakening of the vibrational intensities of the features near 1100 cm^{-1} and 1590 cm^{-1}, which correspond to the B-C stretching vibration and the C-B-C chain stretch, respectively. Infrared spectra of the ground boron carbide are sharper and more intense relative to as received material.

ACKNOWLEDGMENTS

Thanks are due to Dr. Jingzhu Hu and Dr. Zhenxian Liu of BNL for their technical assistance. Use of the National Synchrotron Light Source, Brookhaven National Laboratory, was supported by the U.S. Department of Energy, Office of Science, Office of Basic Energy Sciences, under Contract No. DE-AC02-98CH10886.

REFERENCES

Aselage, T. L., and Emin, D., 1991: Structural Model of the Boron Carbide Solid Solution, in *Boron-Rich Solids*, Ed. D. Emin, T. L. Aselage, A. C. Switendick, B. Morosin, and C. L. Beckel, American Institute of Physics, New York, 177-185.

Bourne, N. K., 2008: The Relation of Failure under 1D Shock to the Ballistic Performance of Brittle Materials, *Int. J. Impact Eng.* **35**, 674-683.

Chen, M, McCauley, J. W., Hemker, K. J., 2003: Shock Induced Localized Amorphization in Boron Carbide, *Science*, **299**, 1563-1566.

Dandekar, D. P., 2001: Shock Response of Boron Carbide, ARL-TR-2456.

Davis, B.L., 1964: X-ray Diffraction Data on Two High-Pressure Phases of Calcium Carbonate, *Science* **145**, 489-491.

Dodd, S. P., Saunders, G. A., James, B., 2002: Temperature and Pressure Dependences of the Elastic Properties of Ceramic Boron Carbide (B_4C), *J. Mats. Sci.* **37**, 2731-2736.

Domnich, V., Gogotsi, Y., Trenary, M., and Tanaka, T., 2002: Nanoindentation and Raman Spectroscopy of Boron Carbide Single Crystals, *Appl. Phys. Lett.* **81**, 3783-3785.

Ge, D., Domnich, V., Juliano, T., Stach, E. A., and Gogotsi, Y., 2004: Structural Damage in Boron Carbide Under Contact Loading, *Acta. Mater.* **52**, 3921-3927.

Ghosh, D., Subhash, G, S., Lee. C. H., and Yap, Y. K., 2007: Strain Induced Formation of Carbon and Boron Clusters in Boron Carbide During Dynamic Indentation, *Appl. Phys. Lett.*, **91**, 061910-1 to 3, and references there in.

Goncharov, A.F., Hemley, R.J., Mao, H.K., and Shu, J., 1998: New High-Pressure Excitations in Parahydrogen, *Phys. Rev. Lett.* **80**, 101-104.

Fanchini, G., McCauley, J.W., and Chhowalla, M., 2006: Behavior of Disordered Boron Carbide Under Stress, *Phys. Rev. Lett.* **97**, 035502-1 – 035502-4.

Hu, J., Mao, H.K., Shu, J., and Hemley, R. J., 1994: High Pressure Energy Dispersive X-ray Diffraction Technique with Synchrotron Radiation, in *High Pressure Science and Technology - 1993* (eds. S. C. Schmidt, Shaner, J. W., Samara, G. A. and Ross, M.) 441-444 (AIP Press, New York, 1994).

Lazzari, R., Vast, N., Besson, J.M., Baroni, S., and Dal Corso, A., 1999: Atomic Structure and Vibrational Properties of Icosahedral B_4C Boron Carbide, *Phys. Rev. Lett.* **83**, 3230 – 3233.

Liu, L.-G., and Mernagh, T.P., 1990: Phase Transitions and Raman Spectra of Calcite at High Pressures and Room Temperatures, *Am. Mineral*. **75**, 801-806.

Liu, Z., Yang, H., Hu, J., Mao, H.K., and Hemley, R.J., 2002: High-pressure Synchrotron X-ray Diffraction and Infrared Microspectroscopy: Applications to Dense Hydrous Phases, *J. Phys: Condensed Matter* **14**, 10641-10646.

Manghnani, M. H., Wang, Y., Li, F., Zinin, P., and Rafaniello, W., 2000: Elastic and Vibrational Properties of B4C to 21 GPa, in *Science and Technology of High Pressure*, Ed. M. H. Manghnani, W. J. Nellis, and M. F. Nicol, University Press, Hyderabad, India, 945-948.

Mao, H.K., Xu, J., and Bell, P.M., 1986: Calibration of the Ruby Pressure Gauge to 800kbar under Quasihydrostatic Conditions, *J. Geophys. Res.* **91**, 4673-4676 .

Schninder, T.L., and Vohra, Y.K., 1995: A Micro Raman Investigation of High-Pressure Quenched Graphite. *J. Phys.- Condensed Mat*. **8**, L637-L642.

Shirai, K., and Emura, S., 1996: Lattice Vibrations and the Bonding Nature of Boron Carbide, *J. Phys. Condens. Matter* **8**, 10919-10929.

Somayazulu, M. S., Akella, J., Weir, S. T., Hauserman, D., and Shen, G., 2001: X-ray Diffraction Measurements on B_4C Boron Carbide at High Pressures and High Temperatures, *Advanced Photon Source Activity Reports.*

Tallent, D.R., Aselage, T.L., Campbell, A.N., and Emin, D., 1989: Boron Carbide Structure by Raman Spectroscopy, *Phys. Rev. B* **40**, 5649-5656.

Vogler, T. J., Reinhart, W. D., and Chhabildas, L. C., 2004: Dynamic Behavior of Boron Carbide, *J. Appl. Phys*., **95**, 4173-4183.

Werheit, H., Au, T., Schmechel, R., Shalamberidze, S.O., Klandadze, G.I., and Eristavi, A.M., 1999: IR-Active Phonons and Structure Elements of Isotope-Enriched Boron Carbide, *J. Sol. State Chem.* **154**, 79-86.

Yan, X.Q., Li, W.J., Goto, T., and Chen, M.W., 2006: Raman Spectroscopy of Pressure-Induced Amorphous Boron Carbide, *App. Phys. Lett.* **88**, 131905-1 – 131905-3.

Zha, C.S., Mao, H.K., and Hemley, R.J., 2000: Elasticity of MgO and a Primary Pressure Scale to 55 GPa, *Proc. Nat. Acad. Sci.* **97**, 13494–13499.

Zhang, Y., Mashimo, T., Uemura, Y., Uchino, M., Kodama, M., Shibata, K., Fukuoka, K., Kikuchi, M., Kobayashi, T., and Sekine, T., 2006: Shock Compression Behaviors of Boron Carbide (B_4C), *J. Appl. Phys.*, **100**, 113536-1 to 5.